

# Influences of powder morphology and spreading parameters on the powder bed topography uniformity in powder bed fusion metal additive manufacturing

**Andre Mussatto, Robert Groarke, Aidan O'Neill, Muhannad Ahmed Obeidi, Yan Delaure, Dermot Brabazon**

School of Mechanical and Manufacturing Engineering, Dublin City University, Glasnevin, Ireland  
I-Form Advanced Manufacturing Research Centre, Dublin City University, Glasnevin, Ireland  
Advanced Processing Technology Research Centre, Dublin City University, Glasnevin, Ireland  
Castolin Eutectic, Magna Business Park, Citywest, Dublin 24, Ireland

Corresponding Author: [andre.mussatto2@mail.dcu.ie](mailto:andre.mussatto2@mail.dcu.ie)

## **Abstract**

Powder spreading is a crucial step in the powder bed fusion process, which controls the quality of powder bed and consequently affects the quality of printed parts. To date, however, powder spreadability has received very little attention and substantial fundamental work is still needed, largely because of the lack of experimental studies. Therefore, the focus of the present study addresses the influences of powder morphology, spreading velocity and layer thickness on the powder bed topography uniformity. The experiments were conducted with a laser powder bed fusion printer and the powder layers were spread systematically and comprehensively assessed. In summary, it was found that particle sphericity and surface texture dictates the degree of impact that the spreader velocity and the layer thickness exert on the quality of powder bed topography in spread layers. The spreader velocity has substantial influence on powder bed uniformity, such that better uniformity is achieved with low spreading velocities,  $\leq 80$  mm/s. Powders with a wide particle distribution and containing large number of fine particles ( $< 25$   $\mu\text{m}$ ) enabled formation of uniform and dense powder beds, however such powders were found to be more affected by segregation. In addition to these observed effects, for the first time, the major process related challenges to powder spreadability and powder bed quality are reported in this study.

## **Keywords**

Powder spreadability, Powder rheology, Particle segregation Selective laser melting, Stainless steel

To cite this article, *Andre Mussatto, Robert Groarke, Aidan O'Neill, Muhannad Ahmed Obeidi, Yan Delaure, Dermot Brabazon, Influences of powder morphology and spreading parameters on the powder bed topography uniformity in powder bed fusion metal additive manufacturing, Additive Manufacturing, Volume 38, February 2021, 101807.*

# 1. Introduction

Selective laser melting (SLM) is as known as the laser powder bed fusion (PBF) technique for metal additive manufacturing (AM) which allows the printing of three dimensional parts by spreading and selectively melting powder in a layer by layer fashion [1]. In comparison with conventional manufacturing techniques, SLM offers near net shape production of complex geometries and capability for pointwise control of microstructure, as well as a high degree of control over the physical and mechanical properties of parts [2], [3]. However, the SLM process is very complex and governed by numerous factors and physical mechanisms [4]. For this reason, substantial research has been conducted in recent years in order to gain further understanding of the underlying physical mechanisms which are strongly material and process parameter-dependant, and ultimately optimise the process and properties of fabricated parts[5]. The powder properties and the powder bed quality are key factors governing the numerous physical mechanisms and hence properties of printed parts [6]. Therefore, it is important to understand how powder is spread across the build area and understand the formation of powder layers, in order to accurately predict powder bed quality [7]. A powder must possess suitable rheology properties in order to form thin, dense and uniform powder layers [8], [9]. However, the ability of a powder to flow well is highly influenced by the shape, size, size distribution, surface texture, porosity, chemical composition, moisture content, density, electrostatic charge and stiffness of its particles [10], [11], [12], [13]. Therefore, powders having values for these and other characteristics inclined towards optimisation of their flowability are preferable [14]. In terms of spreadability, a powder which has ideal flow characteristics for SLM does not alone ensure the formation of good quality powder layers, as spreadability is also governed by other factors such as spreader speed, spreader pressure, spreader material type and powder temperature. Nonetheless, flowability is an essential powder property towards the achievement of uniformly spread powder layers [15].

The powder spreading process is also governed by the spreader system (roller or blade), spreading parameters, powder supply factor and powder layer thickness [16]. During powder spreading, particles undergo particle-particle and particle-spreader interactions which can lead to electrostatic charging and particle morphological changes, which can prevent the formation of high quality powder layers [17], [18], [19], [20], [21]. The spreading of powder onto a non-uniform and unstable layer which was previously spread and a very rough built surface as well as the presence of large spatter particles on the powder bed can be challenging for the formation of uniform consecutive layers. Additionally, the powder bed can also be affected by the inert gas flow system which functions to remove by-products and ensure a safe process atmosphere. An excessive flowrate and velocity of inert gas has been shown to remove particles from spread layers and hence compromise the powder bed quality [22], [23], [24], [25].

Recently, it was reported the lack of standard test methods for spreadability that provide guidance for quantitative assessment of powder spreadability [26]. Unfortunately, today measuring and quantifying powder spreadability is identified as a crucial knowledge gap in the SLM process [27]. However, research efforts are now being seen in this area in terms of in situ investigations and simulations. Nevertheless, there exist numerous challenges such as complex part architecture, rough environment inside the building chamber of SLM systems and the lack of physical results against which to validate powder spreading simulations.

The discrete element method has been a useful numerical tool for studying powder flow dynamics in PBF AM [28]. Recently, it has been also exploited by a number of researchers to study powder spreading dynamics. A recent study reported that a small amount (vol%, 1.5) of fine particles ( $20\ \mu\text{m} < d < 40\ \mu\text{m}$ ) added to the baseline powder ( $45\ \mu\text{m} < d < 150\ \mu\text{m}$ ) can slightly improve the quality of the powder bed in terms of packing density and surface

roughness. However, the spreadability increased and then decreased with adding fines [29]. It was also reported that powders with mean diameter  $\leq 17 \mu\text{m}$  are highly influenced by cohesive forces such that it dominates the gravity forces. The use of such powders resulted in the formation of powder layers of poor quality [30]. Chen et al. concluded from their study that the influence of Van der Waals force rises and dominates with increasing fine particle content. This also resulted in poor powder flowability and in turn powder spreadability. On the other hand, powders with particle radius  $> 21.8 \mu\text{m}$  were more favourable for powder flowability and presented lower particle friction coefficients, resulting in a denser and more uniform powder bed layer [31]. In terms of spreaders, Haeri utilised discrete element method simulations to optimise the geometry of blade spreaders while assuming a super elliptic edge profile and varying its height, width and overall shape. The results showed that the optimised blade can generate a bed with packing density very close to roller systems and can translate to higher production rate (velocity) than the non-optimised blade with limited impact on the powder bed quality [32]. However, to fully demonstrate the effectiveness of the optimised blade design, it should be tested on an actual PBF system. In a different study, the spreading of non-spherical particles was also simulated using the discrete element method [33]. The results suggested that larger particle aspect ratios or higher spreader translational velocities resulted in smaller packing density and higher surface roughness of spread layers. Therefore, this study highlights the importance of particle sphericity and spreader velocity on the quality of powder bed. Nan et al. investigated the effect of layer thickness on transient particle jamming using discrete element method simulations [34]. They found that small layer thicknesses are influenced by powder segregation and can form empty patches on spread powder layers due to particle jamming. The collapse of jammed particles during spreading was then reported in some instances to lead to the particle burst into the spreading layer, deteriorating even further spread layers.

Other studies focused purely on the experimental side of powder spreadability. Snow et al. developed a powder spreadability test rig to assess powder spreadability. They reported that the angle of repose is one of the most influential input factors in powder spreadability. Powders with lower angle of repose were more flowable and provided higher deposition rate, whereas powders with high angle of repose formed a poor powder coverage and powder aggregates. Increasing the spreader velocity from 50 to 150 mm/s increased the powder deposition rate. However, those powders with angle of repose  $> 40^\circ$  exhibited poor flowability for high spreading velocities and based on the rate of change of the avalanching angle were unable to improve spreadability [27]. Another study investigating the effect of powder moisture on spreadability reported that powder morphology had a large influence on moisture absorption and flow behaviour. From the investigated powders, Aluminium alloys were found to be extremely sensitive to oxygen and moisture uptake in comparison to Inconel and titanium alloys. The spreading of moisture-containing powders showed their tendency for agglomeration formation and segregation of particles during the spreading. Additionally, the authors also reported that the spreading of such powders was characterised by scratches on the powder bed [35]. Lerma et al. concluded from their study that powders with morphological characteristics towards sphericity and surficial smoothness led to an almost 50% increase in packing density. In addition, they also reported particle segregation during the powder spreading. Large particles segregated near the beginning of spreading while smaller particles segregated towards the end of the build platform [36]. However, another study reported the opposite segregation behaviour and found higher packing densities near the beginning of spreading and a decline of the packing density near the end of the build platform [37].

The reviewed literature demonstrates the importance of powder spreadability for PBF systems and the influence of various powder characteristics, spreading parameters and intrinsic mechanisms on the powder bed quality. To date, powder spreadability has received very little attention, with conflicting observations. Therefore, substantial fundamental work on this topic

is still needed. Hence, experimental approaches are the best way forward to thoroughly understand spreadability and validate numerical models. The focus of the present study addresses the influences of powder morphology, spreading velocity and layer thickness on the powder bed topology uniformity. Briefly, the powder samples underwent a series of investigations to enable the correlation of their characteristics to their observed spreadability. A three-level full factorial design was employed in order to obtain a comprehensive understanding of the influence of each of the three factors and their levels on the powder bed topographical quality. Uniformity, profile height and profile void volume were studied from the powder bed topography. Additionally, particle segregation and process inherent challenges were examined and are presented in order to expand the understanding of powder spreadability and its implications to part quality.

## 2. Materials and methods

### 2.1. Powder characterization

Three AISI 316 L stainless steel powders obtained from Alfa Aesar (powder A), not supplied for metal AM, and from Castolin Eutectic (powder B) and Carpenter Additive (powder C), which were designed for metal AM. The powders physical characteristics were analysed using a scanning electron microscope (SEM) Zeiss EVO LS-15 and a Malvern Mastersizer 3000 particle size analyser. A Micromeritics AccuPyc 1330 Helium Pycnometer was used to assess the density of the powders, and the flow properties of the powders were investigated using a Freeman FT4 powder rheometer. The powders angle of avalanche was measured using the in-house developed system based on the Revolution Powder Analyzer and the angle of repose was measured using the Hall Flowmeter funnel set up as recommended by the ASTM F3049 standard [38], [39].

### 2.2. Powder spreading and experimental design

In order to ensure the relevance of the spreadability test to the actual laser PBF process, the experiments were conducted inside the laser PBF build chamber of an Aconity Mini (Aconity3D, Germany). To minimise the electrostatic charging of the powder during the spreading process, the powder spreader system of the printer was fitted with an anti-static carbon fibre brush. A powder supply factor typical of metal AM processing on the Aconity of two was employed which means that twice the amount of powder required for the set layer thickness was spread. This was to ensure that there is enough powder to cover the printing area while avoiding excessive and unnecessary use of powder. The experiments were conducted using extreme parameter levels as well as levels that are typically used in powder bed metal printing (as per the design illustrated in Table 1) in order to understand the effect of the various powder morphologies, rheological characteristics and spreading parameters on the spreading of uniform powder beds. A 20 mm by 20 mm by 5 mm depth container was placed within the powder bed to capture the powder bed samples. This was filled with powder while embedded within the powder bed. When filled, a further five layers of powder were spread according to the automated spreader operation. The sample container was then carefully extracted in order to not disturb the powder surface before surface profile measurement.

**Table 1.** Experimental design.

Sample	Run	Layer thickness ( $\mu\text{m}$ )	Spreader velocity (mm/s)	Powd
1	17	70	160	C
2	22	50	160	C
3	4	30	160	C
4	12	70	80	C
5	6	50	80	C
6	14	30	80	C
7	16	70	10	C
8	25	50	10	C
9	18	30	10	C
10	13	70	160	B
11	21	50	160	B
12	27	30	160	B
13	11	70	80	B
14	24	50	80	B
15	8	30	80	B
16	26	70	10	B
17	1	50	10	B
18	10	30	10	B
19	20	70	160	A
20	9	50	160	A
21	23	30	160	A
22	3	70	80	A
23	15	50	80	A
24	5	30	80	A
25	2	70	10	A
26	19	50	10	A
27	7	30	10	A

### 2.3. Powder bed topography assessment

Precise measurement of the spread powder topographies was conducted using a Keyence VHX2000E optical 3D digital microscope. A magnification of 300x was found to be suitable for this analysis as it enabled a good balance between area of coverage and degree of detail visible. The set-up for a depth resolution of 1  $\mu\text{m}$  was employed in order to accurately capture and report the topographical characteristics of powder bed samples such as peaks, pores and agglomerations. Eight profile measurements within this area of 800  $\mu\text{m}$  by 1102.3  $\mu\text{m}$  were taken for each powder sample, which was based on the sample original area. This was to measure powder bed topography variations to allow to draw a more precise conclusion about

the investigated parameters. The sample size,  $n$ , was chosen based on the profile void volume and profile height responses as per equation  $n=(1.96\sigma/e)^2$ , where  $\sigma$  is the standard deviation and  $e$  is the sampling error.

## 2.4. Particle segregation evaluation

Powder C was used in this study as it has better all-around properties (physical and flow) and because it performed better than powder A and B in the spreadability studies. 100 layers each having 50  $\mu\text{m}$  thickness were spread with a powder supply factor of two using a spreader velocity of 80 mm/s. The powder samples were then collected from the begin, middle and end of the build platform and assessed using the Malvern Mastersizer 3000 particle size analyser.

## 2.5. Morphologies challenging powder spreadability

Four  $5 \times 5 \times 5$  mm cubes were printed using the parameters of sample five, [Table 1](#). The Aconity Mini (Aconity3D, Germany) laser PBF machine was used to print these samples. The hatch spacing was held constant at 60  $\mu\text{m}$  and the focus diameter was set to 80  $\mu\text{m}$ . The parts were exposed with a laser power of 140 W at a scanning speed of 800 mm/s. Argon was used as protective gas and the oxygen content inside the chamber was kept below 50 ppm. The morphology of the powder bed with the printed samples were then investigated using a Keyence VHX2000E optical 3D digital microscope.

# 3. Results and discussion

## 3.1. Powders morphology and flow characteristics

The three powders investigated in this study are shown in the images in [Fig. 1](#). Powder A is deemed morphologically unsuitable for selective laser melting. The reason for using this powder was to help to assess the spreadability of the other two powders. This powder consists of nonspherical and elongated irregularly shaped particles. On the contrary, powder B has a good particle sphericity and a small number of elongated particles. However, its particles present a consistent surface texture. Powder C has a higher degree of sphericity. However, irregular, fines and satellite particles are present. The optical images to the right handside of the micrographs show the pouring characteristics of each of the powders. Powder A presented poor flowability for PBF applications mainly due to substantial particle mechanical interlocking. The flowability of powder C also seems to have some degree of restriction due to particle mechanical interlocking. However, powder B apparent to be a free flowing powder.

The particle size distributions of the powders under investigation are shown in [Fig. 2](#). As expected, powder A has the wider particle size distribution. It is comprised of very large particles ( $\approx 100 \mu\text{m}$ ) and a considerable number of fines. Powder B presented a gaussian type of distribution which is generally considered optimal for the SLM process. A similar distribution is seen in powder C. However, the distribution is shifted to the left and approximately half of the particles contained in this powder is sized below 30  $\mu\text{m}$ . Fine particles ( $< 20 \mu\text{m}$ ) are known to have a

tendency for agglomeration and high level of cohesiveness therefore impacting on its powder flowability.

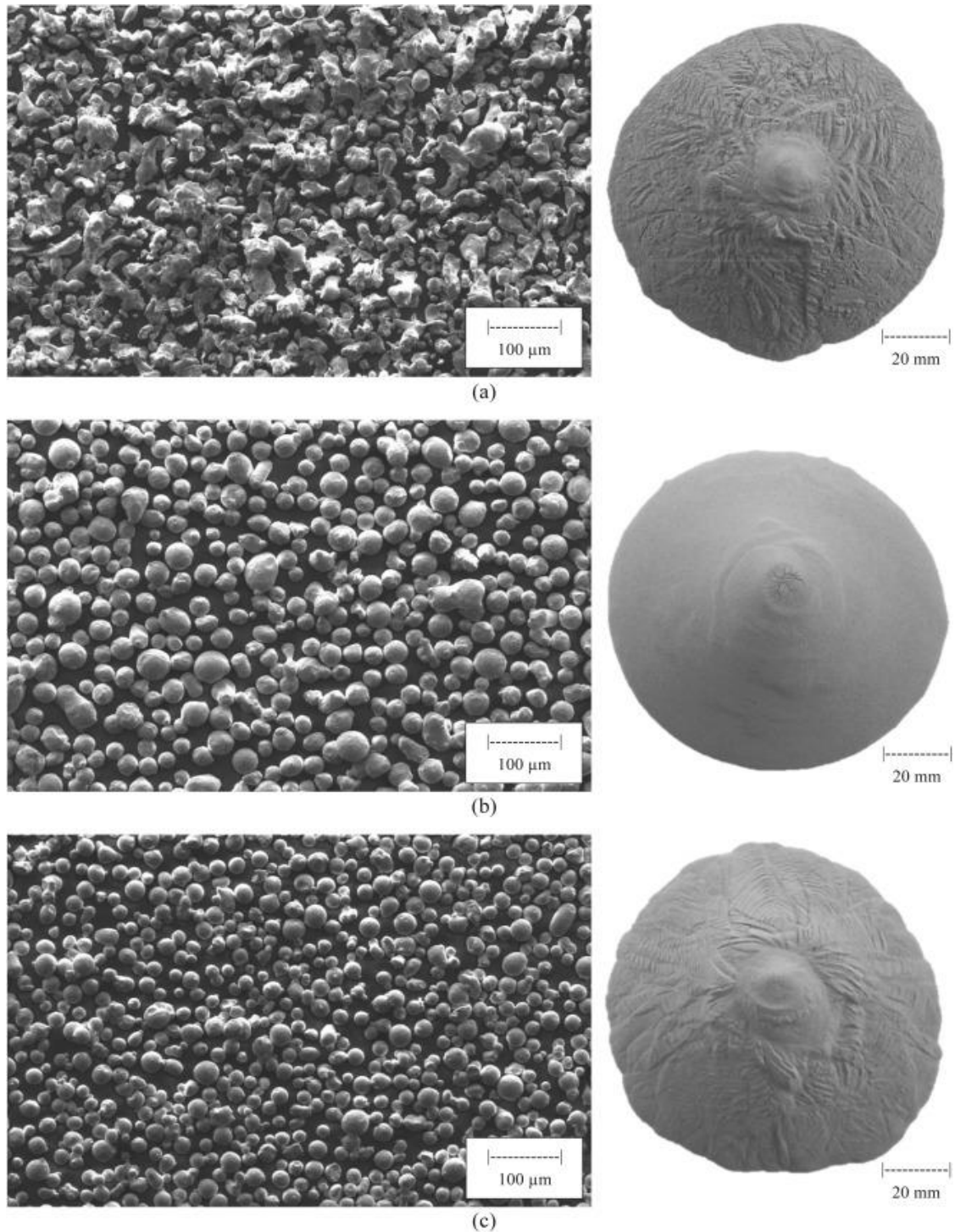


Fig. 1. SEM micrographs of the 316 L stainless steel powder (a) A, (b) B and (c) C. The optical images on the right hand side compares the pouring characteristics of the powders.

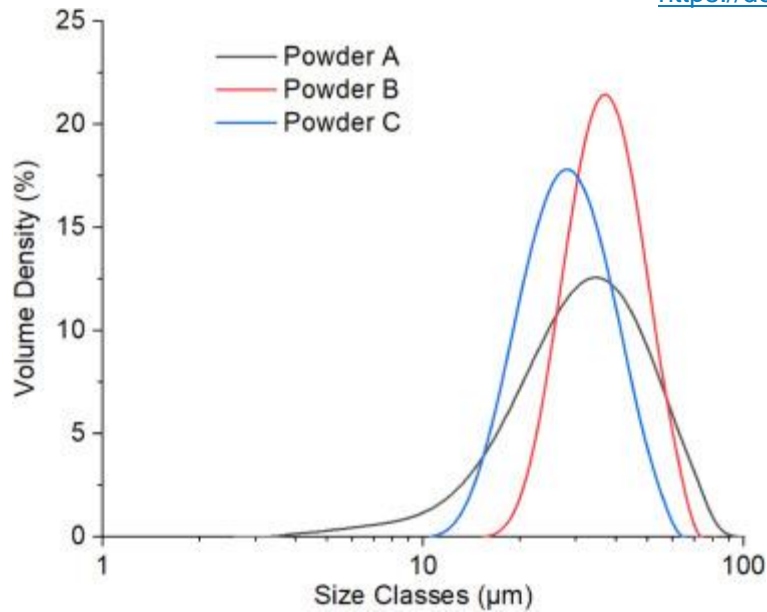


Fig. 2. Particle size distribution of the powders, as measured by laser diffraction.

Table 2 compares the morphological, physical and rheological characteristics of the powders that are fundamental for understanding their spreadability. The up and down arrow directions seen in the table indicate the favourable trend to maximise spreadability. Powder B and C presented similar circularity (circularity is a measure of the particles sphericity). However, Powder C presented 10% higher sphericity than powder B and this can be considered an advantage towards a better flowability. In addition, powder C also presented the best length to width relationship (aspect ratio). This is also seen in the micrographs of Fig. 1. The effect of particle morphology on the bulk density of the powders is seen in Table 2. As shown by the bulk density measurements, powder A presented a large void volume fraction of packed powder, whereas the spherical powders B and C were seen to achieve a more efficient packing. The avalanche and repose angle results suggest that the flowability of powder A is largely restricted by its irregular particles morphologies. Therefore, this powder lacks in a vital requirement for achieving good powder spreadability. On the other hand, both powder B and C presented very similar angles to those powders suitable for PBF [40]. The specific energy measurements which were obtained assuming flow in a low stress environment identified powder B as having the lowest cohesion in comparison to the other two powders. This is mainly because of its superior physical properties such as particle size, shape and texture. All the three powders presented low flow rate sensitivity. However, powder B presented the lowest sensitivity to flow rate and there is enough evidence to suggest that this is related to its free flowing behaviour and to the fact that its particles are slightly coarser. Furthermore, identifiable from the powder particle micrographs, the particle surface smoothness of powder B particles was key in determining this powder flowability.

Table 2. Comparison of the important morphological, physical and rheological characteristics of the powders for spreadability.

Measurement	Powder A	Powder B	Powder C	Instrument
Size, $Dv_{90}$	55.5 $\mu\text{m}$	61.6 $\mu\text{m}$	42.4 $\mu\text{m}$	Malvern particle sizer
Size, $Dv_{50}$	31.8 $\mu\text{m}$	36.7 $\mu\text{m}$	28.0 $\mu\text{m}$	
Size, $Dv_{10}$	15.6 $\mu\text{m}$	25.7 $\mu\text{m}$	18.3 $\mu\text{m}$	
Circularity, $\uparrow$	0.37	0.76	0.87	SEM/ImageJ
Elongation, $\downarrow$	0.40	0.22	0.09	
Helium Density	7.77 $\text{g/cm}^3$	7.81 $\text{g/cm}^3$	7.83 $\text{g/cm}^3$	Pycnometry
Bulk Density	2.85 $\text{g/cm}^3$	4.36 $\text{g/cm}^3$	4.56 $\text{g/cm}^3$	FT4
Specific Energy, $\downarrow$	3.10 $\text{mJ/g}$	1.86 $\text{mJ/g}$	2.51 $\text{mJ/g}$	Powder
Flow Rate Index, $\downarrow$	1.09	1.05	1.18	Rheometer
Avalanche Angle, $\downarrow$	54.6°	36.1°	38.5°	Rotating Drum
Repose Angle, $\downarrow$	48.2°	30.3°	28.2°	Hall Flowmeter

## 3.2. Powder bed topography

### 3.2.1. Profile height

The profile height measured from the powder bed topography quantified the difference between the lowest valley to the highest peak of powder. Hence, it is an indication of the non-uniformity of a powder layer height which due to lack (valleys) and excess (peaks) of powder. When present in excess these defects are typically found in large quantities and randomly dispersed over the powder bed area. A powder bed having a high profile height would certainly lead to problems such as discontinuous and variable meltpool volumes and defects due to lack of fusion. Therefore, to avoid these and other resulting problems the profile height should be as close to 0  $\mu\text{m}$  as possible. The profile height measured from the various powder beds, which were generated using the conditions of Table 1 is shown in Fig. 3. Samples 19–27 correspond to Powder A. The effect of this powder's morphology on the profile height is clear. Therefore, based on the results found for powder B and C, it can be said that particle sphericity and smoothness are significant factors in powder flowability and thus they enabled the formation of more uniform powder layers. However, this is more evident for those samples of powder C, namely samples 3, 4, 5 and 9. The results from these samples suggest that the layer thickness and spreader velocity have a large influence on the profile height. Therefore, it can be said that these two parameters are very relevant for powders with high flowability.

### 3.2.2. Profile void volume

The profile void volume measured from the powder bed topography was defined in this study as the volume required to fill out the valleys up to the highest peak of the powder profile. Fig. 4 shows the profile void volume measured from the investigated area ( $800 \times 1102.3 \mu\text{m}$ ) of the powder bed samples. The high profile void volume obtained from the samples of powder A can be correlated to its particles shape and roughness which caused

substantial mechanical interlocking and interparticle friction during the spreading. When particle morphology is more spherical (powders B and C), mechanical interlocking is less influential as particles are more likely to glance past one another during spreading. However, their net interaction is still influenced by mechanisms such as friction and static charges, which one are also highly influenced by the spreading conditions. In contrast, the below powder samples 4, 5, 8 and 9 presented the lowest profile void volume and this is mainly because Powder C has better all-around characteristics (sphericity, size distribution, texture, etc.) for spreadability and consequently reduced net interaction.

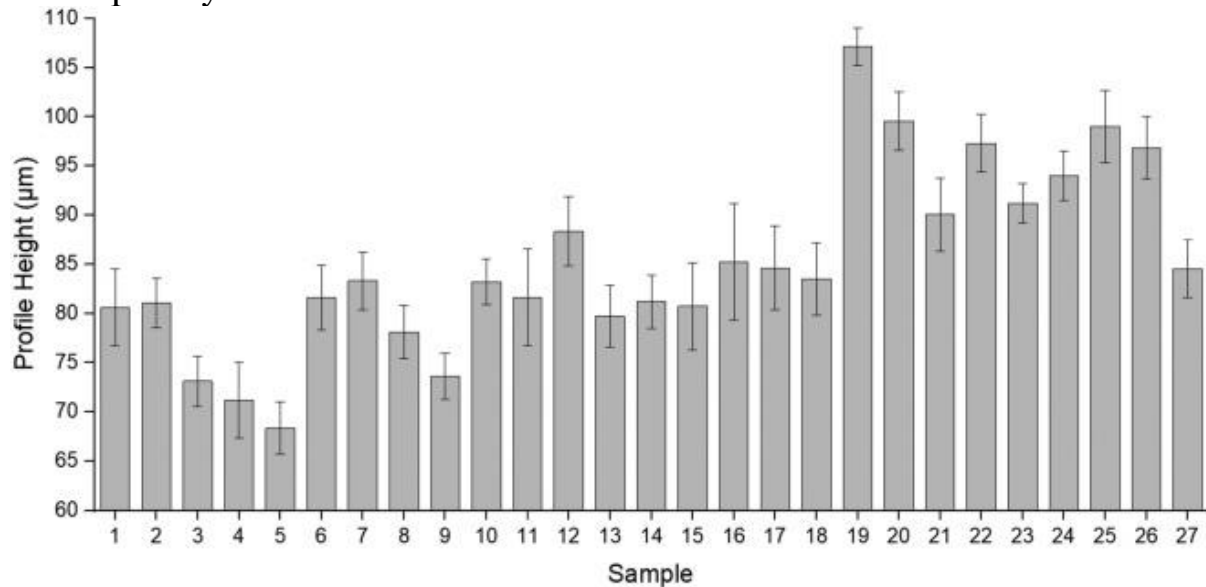


Fig. 3. The maximum profile height measured (from the lowest valley to the highest peak of powder) from the powder bed topography,  $n = 8$ .

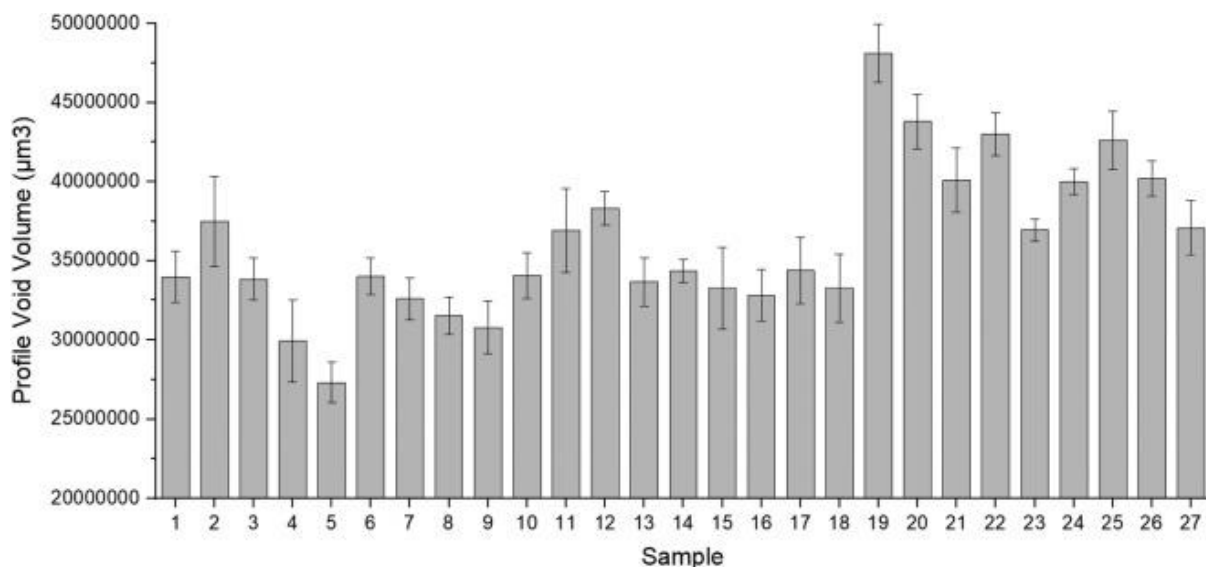


Fig. 4. The profile void volume measured from the powder bed topography (the volume of powder required to fill out valleys with powder up to the highest peak of powder),  $n = 8$ .

Analysis of variance (ANOVA) was used to assist in understanding the fundamentals of powder spreadability, to evaluate the influence of the

parameters on the profile void volume and to find a way to further reduce the profile void volume within the powder bed topography. The analysis was performed using the commercial Design-Expert software v11. Table 3 shows the summary of the ANOVA. The F-value of 10.98 implies the model is significant. There is only a 0.01% chance that an F-value this large could occur due to noise. P-values less than 0.05 indicate model terms are significant. The Predicted  $R^2$  is in reasonable agreement with the Adjusted  $R^2$ , the difference is less than 0.2. The Adequate Precision measures the signal to noise ratio, and a ratio greater than 4 is desirable. The obtained ratio of 11.312 indicates an adequate signal.

Table 3. ANOVA for 2FI model of the profile void volume.

Source	Sum of squares	df	Mean square	F-value	P-value	
Model	4.99E + 14	9	5.55E + 13	10.98455	1.74E-05	significant
A-Layer Thickness	5.77E + 12	1	5.77E + 12	1.142889	0.299988	
B-Spreader Velocity	5.74E + 13	1	5.74E + 13	11.37335	0.003617	
C-Powder	3.9E + 14	2	1.95E + 14	38.65011	4.74E-07	
AB	6.13E + 11	1	6.13E + 11	0.121444	0.731753	
AC	4.41E + 13	2	2.2E + 13	4.365363	0.02951	
BC	9.71E + 11	2	4.86E + 11	0.096154	0.908814	
Residual	8.58E + 13	17	5.05E + 12			
Cor Total	5.85E + 14	26				
Fit Statistics	Value					
$R^2$	0.853272					
Adjusted $R^2$	0.775593					
Predicted $R^2$	0.701581					
Adequate Precision	11.31158					

Fig. 5(a) shows the impact on the profile void volume when spreading with an irregular shaped powder. The plot suggests that lower layer thickness and spreading velocities favour profile void volume reduction. However, a such trend only exists because of three factors; low layer thicknesses ( $< D_{50}$  size of

the powder) restrict the spread of large particles, lower spreading velocities aid the spread of the powder's fine particles first and the fact that the spreader transported twice the volume of powder that is actually required to form the layer. Powder B and C, due to their greater sphericity, showed substantial reduction in profile void volume on their powder bed topographies. When correlating the results presented in [Fig. 1](#) and [Table 2](#) with the results of [Fig. 5\(b-c\)](#), the following can be said. Powder B displayed superior rheological performance. However, Powder C enabled the spreading of layers with lower profile void volume. This is due to its wider particle size distribution and higher number of fine particles. However, it is seen that as the amount of fine particles increases the effect of layer thickness on spreadability decrease. Furthermore, the results suggest that the spreading velocity has substantial influence on the profile void volume, where low spreading velocities ( $\leq 80$  mm/s) resulted in profile void volume reduction.

### **3.2.3. Layer uniformity**

This particular study focused on providing an understanding of the powder spreadability process step which is difficult to quantitatively analyse. The uniformity of the powder bed topographies was determined by assessing the ratios between powder peaks and valleys and their dispersion on the powder bed. The images of the powder bed samples can be found in the [supplementary material](#). [Fig. 6](#) shows the results of this study. There is no clear evidence of interrelation of the parameters at any of the three levels. It can be said that the three powders appear to be similarly influenced by interparticle forces. Furthermore, the powders arrangement behaviour is also influenced by the particle size and particle morphology. Therefore, from the three powders, powder C appears to be slightly less influenced, potentially due to its better all-around morphological properties. Nevertheless, to better comprehend such behaviour of particles when forming powder layers, further studies enveloping a broad range of influencing factors is required.

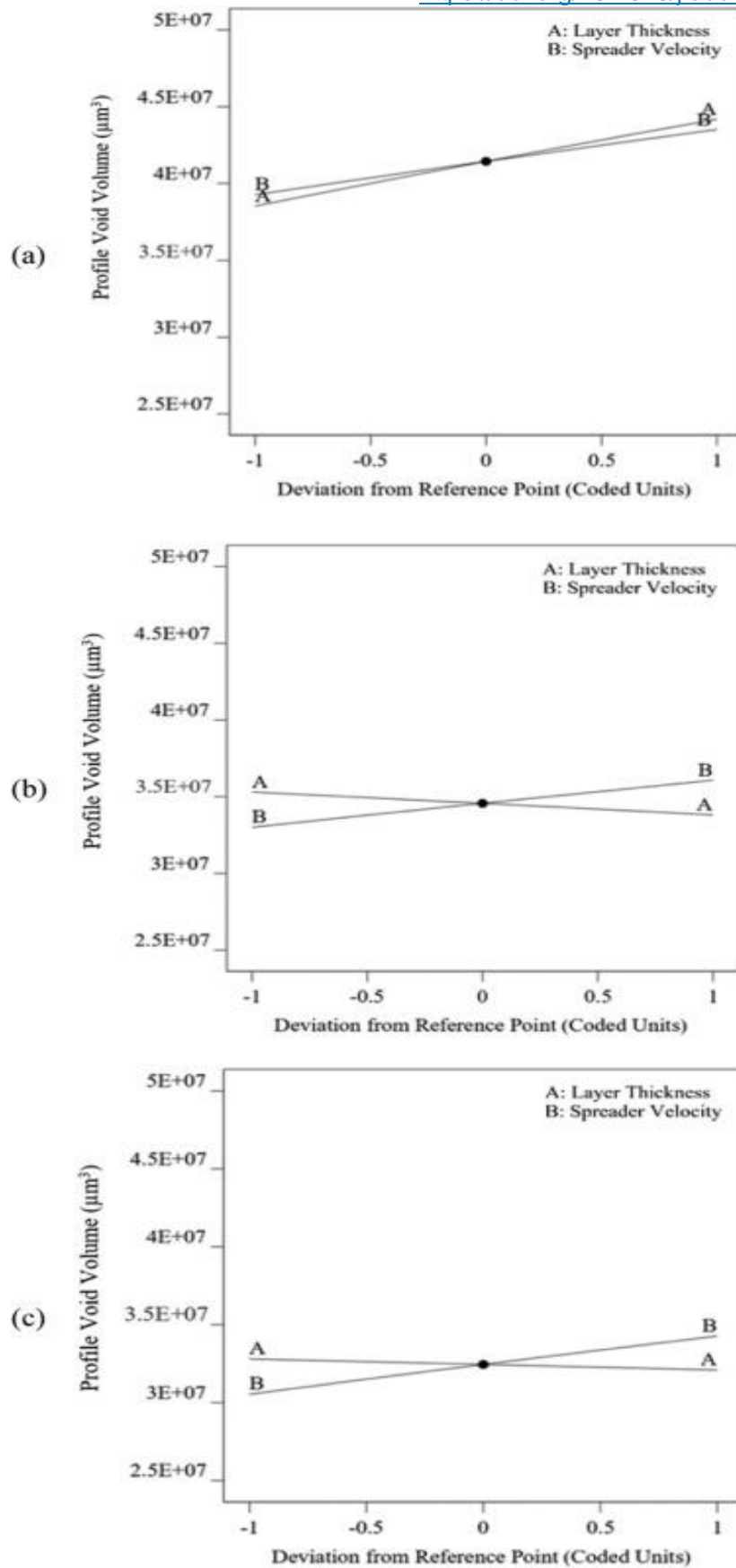


Fig. 5. Summary of the analysis of variance showing the effect of each factor on the profile void volume of the powder bed topography for powder (a) A, (b) B and (c) C.

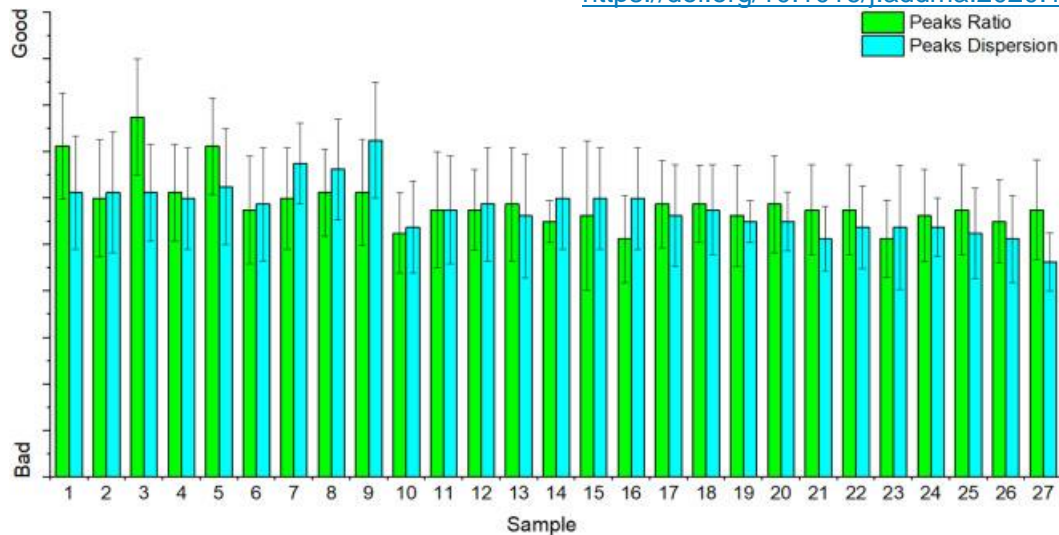


Fig. 6. Ratio between peaks and valleys and their dispersion in the powder bed topography,  $n = 8$ . Peak ratio is the ratio between peak count and valley count. A good peak ratio has equal count of powder peaks and valleys. Peak dispersion refers to the dispersion of powder peaks. A good peak dispersion is when peaks and valleys are dispersed uniformly.

### 3.2.4. Factors affecting the results

The three commercial powders used in this study were supplied having the same particle size distribution. Still, prior to carrying out the experimental work, these powders underwent sieving to remove the variable of different particle size distribution to enable an accurate study of the investigated factors and correlation between their physical and flow characteristics. However, as seen in [Fig. 2](#) there was still exist a small difference between the powders particle size distributions and their volume densities. As can be seen, it is difficult to remove these two variables completely when comparing powders. Nevertheless, their influence on the responses can be minimised via sieving as addressed in this study.

An anti-static carbon fibre brush was used in the spreading of the powders to minimise any static charge within the spreading mechanism from being transferred to the powder particles. However, almost all of the PBF machines and the one used in this study have their chamber and spreading mechanism protected with an anti-static coating material. The carbon fibre type of brush is often used and for very specific applications and in this study it was chosen and used to reinforce the anti-static barrier from the spreading mechanism to the spreading particles. Therefore, the results presented here are also applicable to other blade materials such as rubber lip.

At the magnification used in this work the microscope provided a repeatability of  $1 \mu\text{m}$ . Investigations into the ability of the microscope to reproduce the same measurement revealed a coefficient of variation (standard deviation/mean) of 0.031 for the profile height and 0.026 for the profile void volume. In summary, the measurement error introduced by the microscope is very small having no significant impact in the reported measurements.

The careful and gentle sample removal from the test bed to the microscope did not show any sign of powder bed disturbance or particles rearrangement. A recommendation for an alternative way of assessing the powder bed topography is the optimisation and incorporation of a system within PBF machine right above the printing area such as an ultrahigh accuracy 3D laser profilometer. For example, the hyperspectral interferometry technique has the potential of covering features small as  $0.025 \mu\text{m}$  and real-time surface inspections [41], [42]. Other non-contact techniques such as ultrasonic and capacitive are also useful for specifying surface parameters [43], [44].

### 3.3. Particle segregation

In order to characterize the uniformity of the spread powder layer, particle segregation resulting from the powder spreading process was also investigated in this study. Fig. 7 shows the particle segregation across the length of the powder bed build platform area. Small particles were deposited preferentially at the start of the build platform (as measured from where the powder spreader crosses into the build area) while larger particles were deposited towards the end of the build platform. In fact, the degree of fine particle segregation and deposition was higher at the beginning than when the spreader reached the middle of the build platform, thereby not leaving as many fine particles within the spreading powder toward the end of the build platform. The points X, Y and Z indicated in Fig. 7 show clearly the preference of the fine particles contained in the powder deposited initially. The effect of such segregation behaviour resulted in a new particle size distribution in the powder bed length between 70 and 140 mm, where the D-values for this region differ from the D-values of the same powder before its spreading. A powder size density ratio between the original and the powder from this last region of the deposition of close to 3:2 resulted as it seen from  $Dv_{10}$  to  $Dv_{50}$  and  $Dv_{50}$  to  $Dv_{90}$ . This is mainly due to percolation segregation occurring within the dynamic powder avalanching during spreading. While small particles move downwards through the mass filling spaces between the large particles and at the same time the larger particles move upwards due to the Brazil Nut effect [45], [46]. It was previously reported that the main contributors to segregation are particle size, particle size distribution, concentration of fines, particle shape and density [47]. However, the layer thickness and the spreading velocity are also considerable contributors to particle segregation [48], [49]. In addition, the results here showed that particle segregation also occurs to those powders with narrow particle size distribution. Therefore, a convenient approach to minimise segregation would be to optimise the spreading parameters and layer thickness as well as strategically position parts on the build platform in areas less affected by segregation. Particle segregation within a powder bed should be avoided as it produces local variations of the powder bed density and can cause process instabilities in terms of meltpool signature [50], [51].

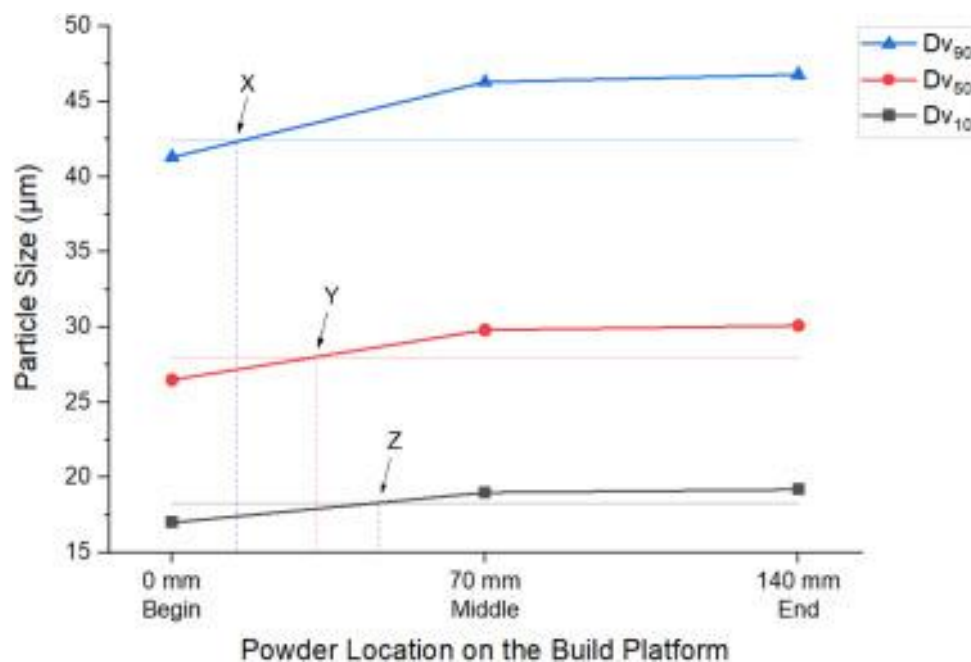


Fig. 7. Particle segregation for powder C in the powder bed measured from the begin to end length of the build platform. The highlighted points X, Y and Z shows the distance from the

begin of the build platform where the D-values of the spread powder equal those of the same powder before the spreading,  $n = 3$ .

### 3.4. Characteristics of laser scanned layers

In selective laser melting, the spreading of powder layers is much more complex than simply spreading one new layer of powder on top of another. Laser processed two-dimensional geometries have very unique textures and laser scanned powder bed layers contain unwanted micro structures inherited from the interaction of the laser with the powder, in addition to other process intrinsic defects. Fig. 8(a) shows spatter particles ejected from the melt pool that fell onto the powder bed. Such spatter particles are likely to become fused with particles from the powder bed. Therefore, when spreading consecutive layers these fused particles can either cause flow separation, be pushed by the spreader scratching the powder bed or cause particle jamming resulting in particles which then collapse and burst into the spreading layer. Fig. 8(b) shows the topography of the powder bed, heat affected particles and the scanned geometry. The spreading of homogeneous consecutive layers in this case is challenging as the volume of powder required to fill the consecutive layer would be different in each of the three zones. In addition, the spreading of powder onto the scanned geometry would certainly lead to localised segregation in the powder bed due to its greater depth. Also, it should be understood that the scanned geometry is fixed to the build platform while particles are loose and the powder bed is compressible. Fig. 8(c) shows the presence of defects on the topography of the scanned geometry. The observed swelling, warping and balling features are common defects in PBF processing geometries. These and similar defects challenge the spreading of subsequent quality layers. The problem with such defects intensifies further when the structures resulting from them pass above the consecutive layer thickness. This is because the contact of the spreader blade with such structures cause localised wear in the blade resulting in non-uniform powder distribution over the powder beds [52]. Defects onto the built surface such as those encountered and reported here can be mitigated by optimisation of the processing parameters such as laser power, scanning speed and hatch spacing as well as using high quality powders [53].

## 4. Conclusions

In this work, the spreadability of metal powders was experimentally investigated using a commercial PBF printer. The effect of powder morphology and the role of the spreading parameters on the quality of powder layer topography is demonstrated in this contribution. To thoroughly understand the influence of the spreading parameters on powder spreadability, a three-level full factorial design was employed. Particle segregation is also reported in this work as well as the major process related

challenges to powder spreadability. The main conclusions from the presented work are summarised as follows:

(1)-The flowability of the highly spherical powder (powder C) containing satellites were slightly lower compared to the less spherical and smoother powder (powder B). This was because of the higher mechanical interlocking of satellite particles, hence naturally resisting to flow. Powders containing large number of fine particles ( $< 25 \mu\text{m}$ ) presented higher specific energy and higher flow rate sensitivity due to the cohesive forces.

(2) The profile height of the powder bed topography is primarily based on the powder flow characteristics, and in this study the profile height was further reduced by optimising the layer thickness and the spreader velocity. Therefore, it can be concluded that these two parameters are very important for powders with high flowability, and deserve careful consideration.

(3) The profile void volume of the powder bed topography is influenced by the powder morphology, spreading conditions and the interaction of the particles. Powder B exhibited higher rheological performance. However, Powder C enabled the spreading of layers with lower profile void volume due to its wider particle size distribution and higher fine particle content. However, as the amount of fine particles increase the effect of layer thickness on spreadability decreases. Furthermore, the results suggest that the spreading velocity has substantial influence on the profile void volume. Where low spreading velocities ( $\leq 80 \text{ mm/s}$ ) resulted in profile void volume reduction. In conclusion, the best uniformity of the powder bed topography was achieved with powder C when spread at  $80 \text{ mm/s}$  in a layer thickness of  $50 \mu\text{m}$ . Based on this, it can also be concluded that the largest particles (D90, and those above it) dictate the minimum layer thickness.

(4) Particle segregation is unavoidable when spreading powders with wide particle size distribution using a spreading blade system. Mitigation of this problem is possible by using tailored powder characteristics (such as particle size distribution, concentration of fines and particle shape) and optimisation of the spreading parameters and layer thickness. Strategically positioning parts on the build platform in areas less affected by segregation also helps to mitigate this problem.

(5) Laser processed two-dimensional geometries have very unique textures and laser scanned powder bed layers contain unwanted micro structures inherited from the interaction of the laser with the powder, in addition to other process intrinsic defects. Therefore, the uniformity and homogeneity of consecutive layers is very complicated to predict well. For this, the relationship of the in-printing characteristics, including scanned geometry, to powder spreadability need to be considered.

The results presented herein are suitable for validating numerical models and they extend beyond the fundamentals of powder spreadability, providing guidelines and recommendations to PBF operators. An accurate prediction of the quality of each spread layer is possible and achievable via powder spreadability simulation coupled with process monitoring. However, for this to come into existence, substantial work is still required around modelling powder dynamics during spreading and a substantial amount of experimental results are needed to validate powder spreading simulations.

The experimental approach used in this work may be referred to as deep powder bed studies (a powder layer spreader onto existing powder layers). Deep powder beds are relevant when printing typically produced parts which contain supports, overhangs, bridges and/or angled facets. The other aspect of powder bed, yet to be researched, is thin powder layer powder spreading (i.e. the spreading of powder layers onto built surfaces). A challenge to this

is that every single built surface will have its own characteristics i.e. roughness and geometry. However, comprehensive studies into both, deep powder bed and thin powder layer will be required in order to acquire powder spreadability data for validating numerical models developed for this process.

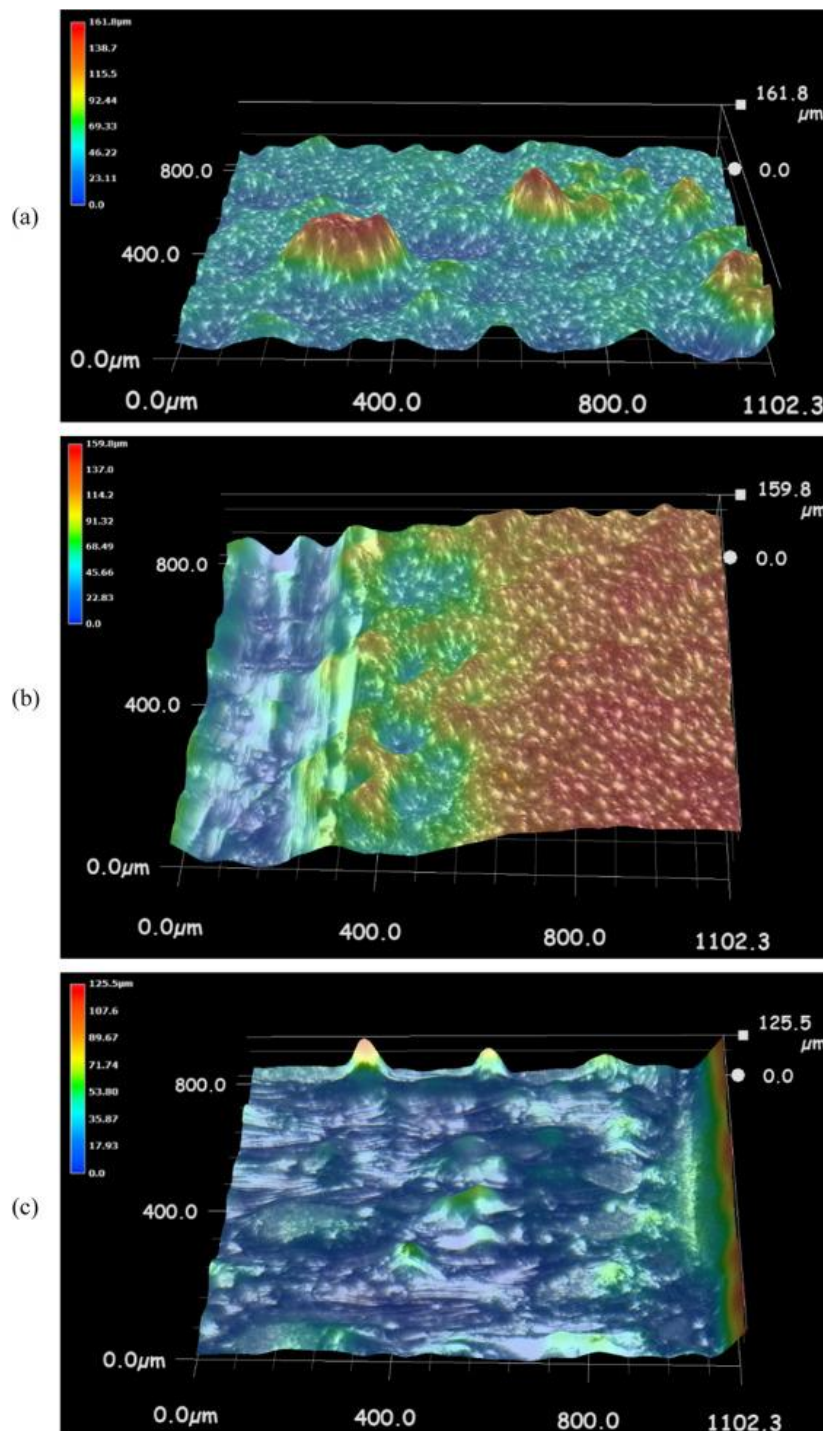


Fig. 8. Morphologies challenging powder spreadability in consecutive layers. Large spatters fused with particles of the powder bed profiling above the layer height (a), Height differences at the interface between the scanned two-dimensional geometry and its powder bed (b) and warping, balling and swelling defects in scanned geometries compromise powder spreadability and the life of powder spreading blades (c).